Optical Scatter—A Diagnostic Tool to Investigate Laser Damage in KDP and DKDP

B. W. Woods *J. J. De Yoreo*

M. Runkel *M. R. Kozlowski*

M. Yan

Introduction

Single crystals of KH_2PO_4 (KDP) and $K(D_xH_{1-x})_2PO_4$ (DKDP) will be used for frequency conversion and as part of a large aperture optical switch[1] in the proposed National Ignition Facility (NIF) at the Lawrence Livermore National Laboratory (LLNL). These crystals must have good optical properties and high laser damage thresholds. Currently, these crystals have a lower laser damage threshold than other optical materials in the laser chain, forcing designers to limit the output fluence of the NIF to avoid damaging the crystals. In addition, minimum acceptable laser fluences can be safely employed only after the crystals have been treated in a procedure known as laser conditioning,[2] which has been shown to dramatically improve their damage thresholds. Furthermore, while more efficient frequency conversion schemes are being explored both theoretically and experimentally, the advantages of these schemes cannot be fully realized unless the damage thresholds of the conversion crystals are increased. Over the past decade, LLNL has generated an extensive data base on laser damage in KDP and DKDP crystals both at the first and third harmonics of Neodymium-doped yttrium-aluminum-garnet (Nd-YAG).[3] Over this time period, the damage thresholds of these crystals have increased, due in part to better filtration of the growth solution;[4] nevertheless, the damage thresholds of the best crystals are still far below the theoretical limits calculated from the band structure of perfect crystals. Thus, damage in KDP and DKDP is caused by defects in the crystals. Unfortunately, little is understood about the mechanism of laser-induced damage, the conditioning process in the crystals, or the defects that are responsible for damage.

Recently, we began an investigation aimed at understanding and improving laser damage and conditioning in KDP and DKDP. Our strategy is to use a range of characterization techniques to profile defects in crystals of both types and to perform damage and conditioning experiments on these well-characterized crystals to identify the defects that are responsible for damage and conditioning. The techniques include ultraviolet absorption measurements for profiling the distribution of impurities, x-ray topography for mapping the locations of structural defects such as dislocations and crystal sector boundaries, and light scattering for detection of inclusions of the growth solution and of foreign particles. This paper focuses on the development and use of light scattering to investigate laser-induced damage in KDP and DKDP. Both types of crystals are very similar in terms of defects and damage thresholds; therefore for clarity in this article, references to KDP include DKDP.

Laser Damage in KDP

Laser damage in KDP typically progresses with increasing laser fluence from pin-point damage characterized by individual 1- to 10-μm-diam damage sites, often with fractures radiating along specific crystallographic directions, to massive damage in the form of a continuous track of 10- to 100-μm diam scatterers visible to the naked eye. Historically, better solution preparation and growth processes have improved the laser damage thresholds in KDP and DKDP. Figure 1 is

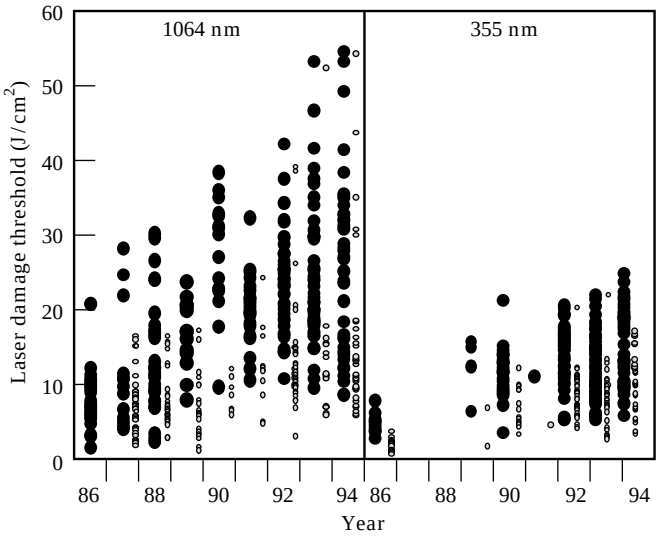

FIGURE 1. Measured bulk damage thresholds vs time for KDP and DKDP, scaled to 3 ns values by $\tau^{0.5}$ and measured at 1ω (1064 nm) and 3ω (355 nm). Note the general improvement in damage thresholds over the 8-year period is shown, as well as the beneficial effect of laser conditioning. Solid circles are conditioned; open circles are unconditioned. (70-50-0296-0307pb01)

a plot of laser-damage thresholds as a function of year measured at 1ω and 3ω for both conditioned (R-on-1) and unconditioned (S-on-1) test conditions. Because damage thresholds are generally measured shortly after growth and fabrication are complete, it is evident that the damage thresholds have improved over time. This plot includes all damage tests on all crystals, so the median values one can deduce are not representative of the best damage thresholds that are currently achieved. For example, the nominal damage threshold for 3-ns pulses at the third harmonic of Nd:YAG in KDP crystals that vendors have produced for the Beamlet laser system[5] are 10 and 20 J/cm^2 for S-on-1 and R-on-1, respectively. While these thresholds could be controlled by typical defects in high-quality crystals such as point defects (impurity atoms) or dislocations, the well-documented improvement in damage thresholds in response to continuous filtration[4] of the growth solution during crystal growth suggests that inclusions play a significant role in damage.

Scatter Measurement

We chose light scattering as a means of characterizing inclusions in KDP. Figure 2(a) is a schematic of the scatter measurement we implemented to view both defects and bulk damage in the crystals. We installed the scatter diagnostic in the ZEUS laser-damage facility at LLNL—a system capable of delivering a usable high-fluence beam of 100 J/cm^2 at 1ω and 75 J/cm^2 at 3ω in an 8-ns pulse. The crystal is mounted in an X–Y translation stage to allow positioning of the damage beam at any point on the crystal. The translation stage is also attached to a rotary stage that allows the test region of the sample to be viewed under an optical microscope, using Nomarski or backlighting techniques to detect damage. This is a typical method used to damage test samples. With the aid of an alignment camera, a probe laser is positioned collinear to the damage beam. To obtain an image of the scattered light from the probe laser, we use a high-dynamic-range 1024 × 1024 pixel, 14-bit CCD camera with appropriate imaging optics to look through the edge of the crystal, horizontally. Current system magnification is approximately 2×, resulting in each pixel mapping to approximately a 10-μm^2 area in the crystal.

Figure 2(b) is a schematic diagram of the illumination and imaging geometry, where the beam propagation is oriented from top to bottom. The nominal beam diameter for the ZEUS damage laser is 1 mm at 1/e^2 of its peak intensity, and the diameter of the probe beam is 2 mm at 1/e^2. We estimate that the two beams are coaligned to approximately ±250 μm at the sample plane. The scatter from the surface has to be avoided because it is much brighter than the bulk scatter and will saturate the camera. Signals we observe consist of several components: Rayleigh scatter, Brillouin scatter, Mie scatter, and fluorescence. Notch filters are used to eliminate the fluorescence and Brillouin signals. The primary focus of this study are Mie scatter sites and scattering off of index variations. The Becke line test[6] has shown that all of the large (Mie) scattering sites we have observed are regions with an index of refraction that is less than the bulk crystal. We have been able to detect many more defects with this scatter diagnostic than with conventional optical microscopy and have seen dramatic differences between different vintages and types of crystals.

Results and Development of Light Scattering

Current studies include four types of crystals with different growth histories. Figure 3 shows the scatter

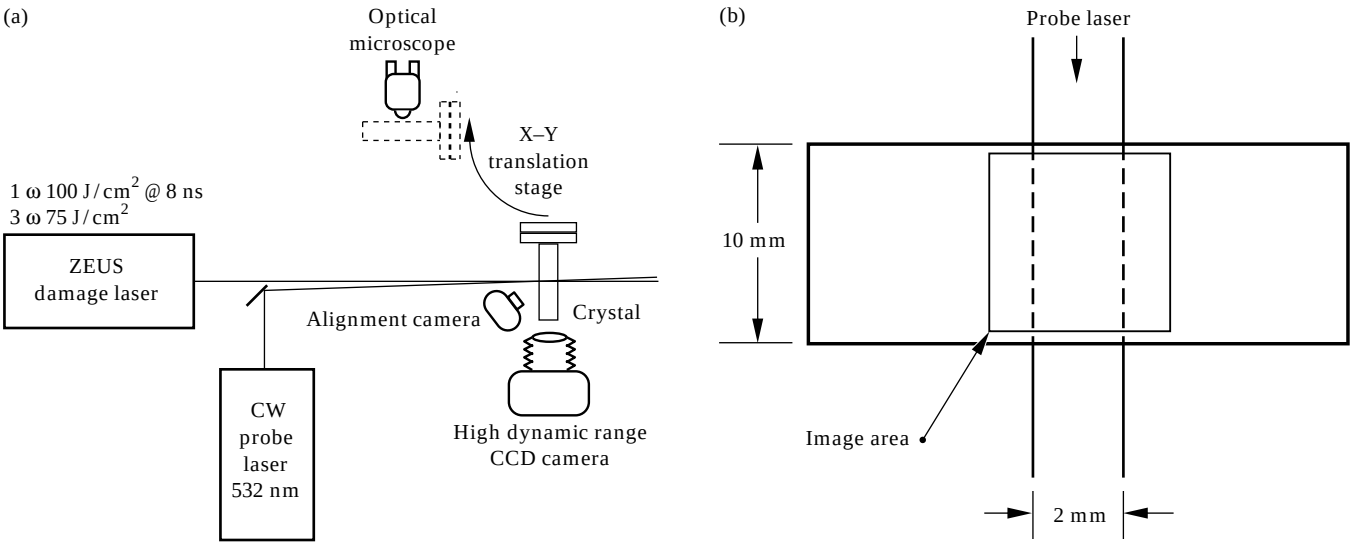

FIGURE 2. Schematic of (a) scatter measurement system and (b) orientation of scatter image. (70-50-1195-2524pb02)

signal from each of these different types—note the gray-scale adjustments for each image to emphasize the important features. Figure 3(a) shows the scatter signal from a crystal grown before continuous filtration increased the damage thresholds.[4] Many large (Mie) scatterers are visible in this type of crystal (currently in use on the Nova laser at LLNL). Figure 3(b) shows a crystal grown later, following improvements in solution processing techniques. These crystals, which are also in use on Nova, have significantly fewer large Mie scattering sites and have a higher laser-damage threshold. Figure 3(c) shows one of the most recently grown crystals used on the Beamlet laser system both in the Pockels cell and as frequency converters. These crystals have very few large (Mie) scattering sites and have the highest laser-damage thresholds of any crystals tested, to date. Figure 3(d) shows a crystal grown at LLNL as part of a program to develop an innovative process for growing KDP and DKDP crystals with excellent optical properties at growth rates up to 10× faster than conventional techniques.[7] This process includes filtration of the solution prior to the start of crystal growth. These crystals have fewer scattering sites than the early Nova crystals, but the sites are typically larger.

During laser-damage tests, we see increases and decreases in the scattering intensity from Mie scatterers. Figure 4 shows a sequence of images in which most of the initial scatter sites diminish in intensity or disappear while one scatter site increases dramatically in intensity, generating what we would traditionally refer to as damage. These images may represent our first glimpse at both the defects that induce damage and the process of laser conditioning. However, while we typically see that nearly all pre-existing scatter sites diminish in intensity or disappear during damage testing, when laser damage occurs, it often does not initiate at an obvious pre-existing scatter site (illustrated in Fig. 5). This unexpected result has four possible explanations: (1) Defects other than inclusions, such as dislocations and point defects, may induce damage. (2) The damage may initiate at features that are below our spatial or intensity resolution. To address this possibility, our detection system currently incorporates microscopy,

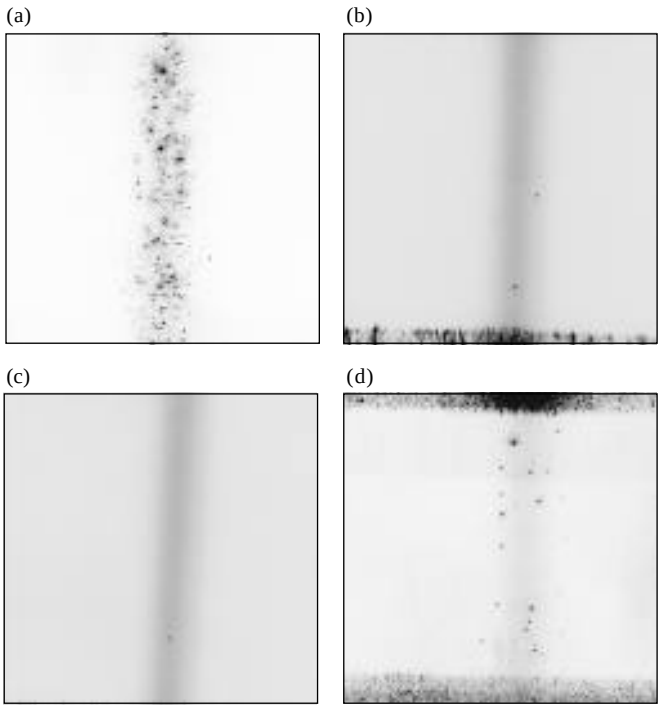

FIGURE 3. Scatter signals from (a) Nova pre-continuous filtration (b) post-Nova, (c) Beamlet, and (d) rapidly grown crystals. (70-50-1195-2525pb01)

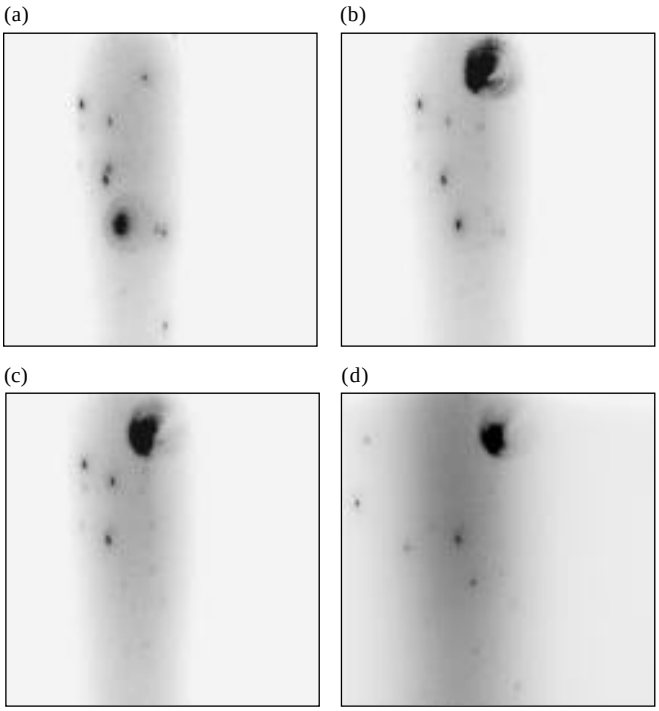

FIGURE 4. Scatter signal from KDP crystal (a) before exposure to the damage beam and after, (b) at one 10.2-J/cm^2 pulse, (c) at one 11.1-J/cm^2 pulse, and (d) at 600 10-J/cm^2 pulses. (70-50-1195-2523pb01)

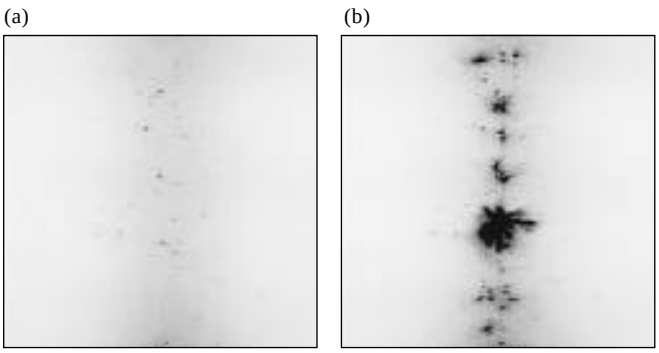

FIGURE 5. Images showing (a) the scatter signal before illumination and (b) heavy laser damage initiated in areas that had no initial scatter sites. (70-50-1195-2526pb01)

allowing us to obtain magnifications of up to 900×. Using these higher magnifications should also help us develop insight into the conditioning process and determine why the amplitude of some scatter sites decreases dramatically when subjected to a high-fluence beam. (3) Damage may be caused not by defects per se but rather initiates in regions that have high stress fields due to defects. Therefore, we plan to develop micrometer-size strain maps for the crystals and to correlate them to optical damage. (4) The illumination angle, viewing angle, or polarization direction of the probe beam might not be optimal to detect the sites where damage initiates.

We investigated item (4) above and found scatter to be quite sensitive to both the angle at which we illuminate the sample and the angle at which we view the scatter signal. Figure 6 shows the scatter signal from a crystal under illumination at normal incidence and at 5° off of normal incidence. The scatter signal from the region near the center of the image nearly disappeared when the crystal was tipped by 5°. This result suggests that there were planar scatterers in the crystals that could only be detected at certain angles. Because KDP grows as a faceted crystal, one might expect to find planar features in the crystals known as growth stria, which lie parallel to the growth front and correspond to variations in growth rate, inhomogeneities in impurity incorporation or sporadic incorporation of particles, and / or solution inclusions. We found that this effect is pronounced in crystal plates cut from the upper portion of KDP boules when the normal to the plate lies along the <001> axis of the crystal, as shown in Fig. 7(a). Such crystals typically contain four separate sectors to which material was added during growth, corresponding to the four {101} faces of the crystal. If the laser is incident normal to the face of the crystal and the camera views the crystal along the normal to one of the edges [see Fig. 7(b)], then the normal to the growth front will be at 45° to both of these directions in one and only one sector. As Fig. 7(c) shows, under these conditions we observed strong scattering with a lineation parallel to the growth front. In other words, we observed scattering from planar variations in the crystal. At the boundary between two adjacent growth sectors, this scattering suddenly disappears and in the adjacent sectors, only Rayleigh and Mie scattering can be observed [see Fig. 7(d) and 7(e)]. Successive rotations of the crystal by 90° result in the same progression of scattering across each of the four growth sectors. Figure 8 shows the scatter

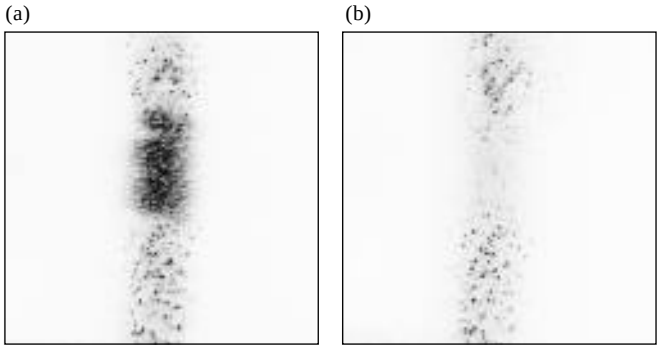

FIGURE 6. Scatter signal from crystal (a) at normal incidence and (b) at 5° from normal. (70-50-1195-2527pb01)

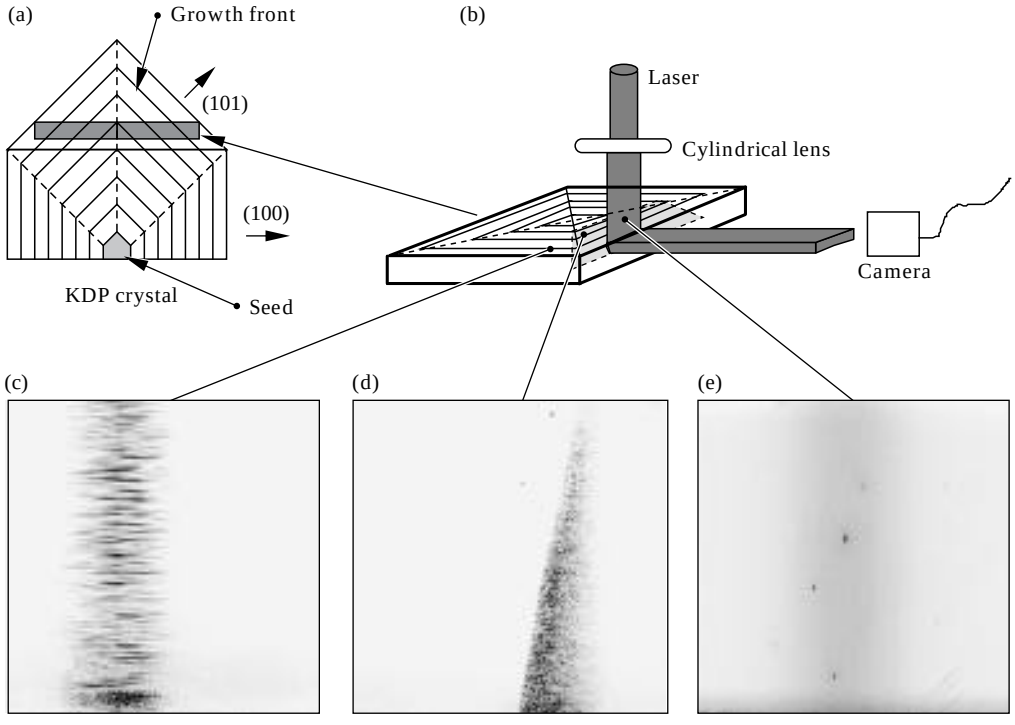

FIGURE 7. Schematic of KDP crystal showing (a) orientation of the growth front relative to plates cut for damage testing, (b) arrangement of laser, crystal, and camera which generates (c) strong scattering from growth planes (d) scattering at sector boundaries, and (e) Rayleigh and Mie scattering only. (70-50-1195-2528pb01)

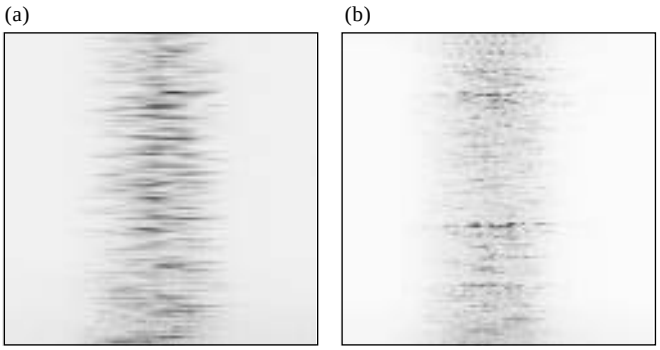

FIGURE 8. Comparison of scattering from growth stria in (a) rapidly grown and (b) Beamlet-vintage crystals. The most intense scattering in (a) is about 20× that in (b). (70-50-1195-2462pb01)

signal generated by these features in a fast-grown crystal as well as one grown for Beamlet. The intensity of the brightest features are about 20 times greater in the fast grown crystal than in the Beamlet crystal. At this time, we do not know if these features consist of planar arrays of inclusions or are simply variations in refractive index which produce a series of dielectric mirrors within the crystal. We also do not know how these features affect the damage threshold of the crystals.

Conclusion

The scatter diagnostic installed on the ZEUS laser-damage facility at LLNL allows us to view scatter and optical damage in bulk KDP. The historical record of damage shows a correlation between the level of filtration and solution processing, number of scattering sites, and optical damage. However, damage often initiates in regions where no initial scatter site is observed. The amplitude of the scatter signal from large (Mie) scatter sites often decreases when subjected to a laser pulse. These sites may be providing our first glimpse into the conditioning process. When the crystals are properly oriented relative to the probe beam and the camera, we observe strong scattering with a lineation perpendicular to the growth direction. We interpret this to be scatter from growth stria—planar variations in crystal homogeneity produced at the growth front of the crystal during growth. Positive identification of the defects that cause laser damage in KDP is crucial to improving damage thresholds for the NIF.

Acknowledgments

We gratefully acknowledge the contributions of Frank Rainer for many helpful discussions regarding laser damage in KDP and for developing an extensive data base on laser-damage measurements at LLNL. We also thank Peter Thelin, Jose Vargas, and Ron Vallene for providing the optical finishing on our many test samples.

Notes and References

1. M. A. Rhodes, B. Woods, J. J. DeYoreo, D. Roberts, and L. J. Atherton, *Appl. Opt.* 34, 5312 (1995).
2. J. E. Swain, S. E. Stowkowski, and D. Milam, *Appl. Phys. Lett.* 41 (1982).
3. F. Rainer, L. J. Atherton, and J. J. DeYoreo, "Laser Damage to Production-and Research-Grade KDP crystals," in *Laser-Induced Damage in Optical Materials*, H. E. Bennett et al. Eds., (SPIE—International Society for Optical Engineering, Bellingham, WA, 1992; *Proc. SPIE*, 1848).
4. K. E. Montgomery and F. P. Milanovich, *J. Appl. Phys.* 68 , 15 (1990).
5. J. Campbell, L. J. Atherton, J. J. DeYoreo, M. R. Kozlowski, et al., *ICF Quarterly Report* 5(1), 52–61, Lawrence Livermore National Laboratory, Livermore, CA, UCRL-LR-105821-95-1 (1994).
6. An Introduction to the Methods of Optical Crystallography, F. D. Bloss, Ed., (Saunders College Publishing, San Francisco, 1989).
7. N. P. Zaitseva, I. L. Smol'skii, and L. N. Rashkovich, *Sov. Phys. Crystallogr* 36, 113 (1991).